frontiers | Frontiers in Astronomy and Space Sciences

ORIGINAL RESEARCH
published: 13 May 2022
doi: 10.3389/fspas.2022.882145

Formamide-Based Post-impact Thermal Prebiotic Synthesis in Simulated Craters: Intermediates, Products and Mechanism

Martin Ferus[1]*, Antonín Knížek[1,2], Lukáš Petera[1,3], Adam Pastorek[1,4], Jana Hrnčířová[1,2], Luboš Jankovič[5], Ondřej Ivanek[1], Jiří Šponer[6,7], Anna Křivková[1,4], Homa Saeidfirozeh[1], Svatopluk Civiš[1], Elias Chatzitheodoridis[8], Klaudia Mráziková[6,9], Lukáš Nejdl[10,11], Franz Saija[12], Judit E. Šponer[6,7] and Giuseppe Cassone[12]*

[1]J. Heyrovský Institute of Physical Chemistry, Czech Academy of Sciences, Prague, Czechia, [2]Department of Physical and Macromolecular Chemistry, Faculty of Sciences, Charles University, Prague, Czechia, [3]Department of Inorganic Chemistry, Faculty of Sciences, Charles University, Prague, Czechia, [4]Faculty of Nuclear Sciences and Physical Engineering, Czech Technical University, Prague, Czechia, [5]Institute of Inorganic Chemistry, Slovak Academy of Sciences, Bratislava, Slovakia, [6]Institute of Biophysics, Czech Academy of Sciences, Brno, Czechia, [7]Regional Centre of Advanced Technologies and Materials, Czech Advanced Technology and Research Institute (CATRIN), Palacky University Olomouc, Olomouc, Czechia, [8]School of Mining and Metallurgical Engineering, National Technical University of Athens, Athens, Greece, [9]National Centre for Biomolecular Research, Faculty of Science, Masaryk University, Brno, Czechia, [10]Department of Chemistry and Biochemistry, Mendel University in Brno, Brno, Czechia, [11]Central European Institute of Technology, Brno University of Technology, Brno, Czechia, [12]Institute for Chemical-Physical Processes, Italian National Research Council (IPCF-CNR), Messina, Italy

Edited by:
Ryan C. Fortenberry,
University of Mississippi, United States

Reviewed by:
Alexander Ruf,
Ludwig Maximilian University of Munich, Germany
Josep M. Trigo-Rodríguez,
Institute of Space Sciences (CSIC), Spain

***Correspondence:**
Martin Ferus
martin.ferus@jh-inst.cas.cz
Giuseppe Cassone
giuseppe.cassone@ipcf.cnr.it

Specialty section:
This article was submitted to Astrobiology, a section of the journal Frontiers in Astronomy and Space Sciences

Received: 23 February 2022
Accepted: 20 April 2022
Published: 13 May 2022

Citation:
Ferus M, Knížek A, Petera L, Pastorek A, Hrnčířová J, Jankovič L, Ivanek O, Šponer J, Křivková A, Saeidfirozeh H, Civiš S, Chatzitheodoridis E, Mráziková K, Nejdl L, Saija F, Šponer JE and Cassone G (2022) Formamide-Based Post-impact Thermal Prebiotic Synthesis in Simulated Craters: Intermediates, Products and Mechanism.
Front. Astron. Space Sci. 9:882145.
doi: 10.3389/fspas.2022.882145

Influx of matter from impacting meteoroids and hydrothermal crater weathering are important factors modifying the rock and mineral inventory of young planets undergoing heavy bombardment. These processes may have influenced not only the geochemical environment of, *e.g.*, early Mars and other planets, but also the peculiar prebiotic chemistry on early Earth. Here, we present a synergistic experimental and computational investigation of the intermediates of chemical reactions of the formamide-based synthesis of canonical and non-canonical nucleobases by thermochemistry in hot hydrothermal crater environments. We put our findings into context with previously investigated plasma-initiated synthesis occuring directly during impact. Both processes result into the formation of all canonical nucleobases, hypoxanthine, purine, and into the onset of the simplest amino acid glycine. Furthermore, it turns out that radical species such as CN and H play a key role in the plasma-assisted impact chemistry. However, post-impact thermochemistry is essential for the origin of formamidine and 2-aminoacetonitrile, intermediate species detected in this study by means of FTIR spectroscopy.

Keywords: prebiotic chemistry, origin of life, formamide, FTIR spectroscopy, quantum-mechanical calculations, ab initio molecular dynamics, metadynamics

1 INTRODUCTION

The origin of life research has gradually shifted towards the identification of geochemical environments favourable for prebiotic synthesis (Hazen et al., 2008; Hazen and Sverjensky, 2010). An influential "Hot Spring hypothesis" proposes that the origin of life may have occurred in hot springs (Damer and Deamer, 2020). This hypothesis lends a central role to intermittent volcanic pools, which provide environment similar to that occurring in impact craters. Violent meteorite impacts represent potentially important energy and material sources deeply modifying the physical and chemical shape of the early Earth and other planets such as, *e.g.*, Mars and Venus. For instance, estimates of the Earth's impact flux prior to ~ 4 Gya suggest an annual energy deposition larger than 10^{20} J (Chyba and Sagan, 1992). Extrapolating such an estimate to Mars by using the impact rates and the velocity scaling taken from the literature (Ryder, 2002; Ivanov, 2008; Schlichting et al., 2012; Abramov and Mojzsis, 2016) leads to 10^{-1} to 10^{-2} times less deposited energy than is expected for Earth. Some contemporary scientists consider Mars an "archive" of planetary evolution. Almost all direct geological information from Earth's Hadean eon is now long lost. Nowadays, the Yarrabubba Crater likely represents the oldest impact structure on Earth (dated back to 2,229 ± 5 Ma) (Erickson et al., 2020). On the other hand, important data is provided by the exploration of Mars, which lacks plate tectonics and at least two-thirds of its present surface is far older (> 3.5 Gya) than Earth's (McKay and Stoker, 1989). Martian surface therefore may preserve traces of processes relevant to prebiotic conditions (Oberbeck et al., 1990; Sasselov et al., 2020), even if life had never existed there.

Some evidence of this preservation comes from martian meteorites. As an example, the Nakhla meteorite contains niche environments exclusively formed during an impact that induced the circulation of hydrothermal fluids which altered the rock and the formed secondary clay and other phases (Chatzitheodoridis et al., 2014). Recent discoveries indicate a strong connection between impacts and the presence of rich organic inventories on the surfaces of early Earth and Mars (*e.g.*, in Chyba and Sagan (1992); Jenniskens et al. (1998); Patel et al. (2015); Pastorek et al. (2019); Erickson et al. (2020); Ferus et al. (2020); Todd and Öberg (2020) and references therein). In particular, the exploration of the Gale crater by the Curiosity rover has confirmed the existence of a relatively complex organic inventory, including chlorobenzene and from C-2 to C-4 dichloroalkanes (Freissinet et al., 2015). Moreover, pyrolysis products of lacustrine mudstones at the base of the 3.5 Ga Murray formation contained thiophenic, aromatic and aliphatic compounds (Eigenbrode et al., 2018). S-bearing species can also be synthesized over Fe/Ni metals in the solar nebula (Llorca and Casanova, 2000, 1998). On Earth, electron paramagnetic resonance (EPR) analysis of 3.33 Ga fossil sediments from the Josefsdal Chert in South Africa shows an anomalous layer of organic matter formed from tiny dust particles. which originate from a flux of micrometeorites falling through the oxygen-poor Archean atmosphere (Gourier et al., 2019). Side processes directly connected with impacts, such as the delivery of possibly reprocessed meteoritic materials (Chyba et al., 1990; Kuwahara and Sugita, 2015), the chemical action of impact plasma (Ferus et al., 2017b; Ferus et al., 2019), hydrothermally-active craters and UV radiation may have played crucial roles in chemical reactions changing the organic inventory present in craters on longer timescales (Sutherland, 2016).

Impact and post-impact synthesis of organic molecules attributed to life's origins might have started from a broad repertoire of prebiotic molecules. However, the apparent relevance of two major starting compounds has enormously increased in the last decade: HCN (Powner et al., 2011; Powner and Sutherland, 2011; Sutherland, 2016; Ferus et al., 2017a; Civiš et al., 2017; Sutherland, 2017; Xu et al., 2017; Ferus et al., 2020) and its hydration product formamide ($HCONH_2$) (Saladino et al., 2012, 2016; Ferus et al., 2015b; Rotelli et al., 2016; Šponer et al., 2016; Cassone et al., 2017; Bizzarri et al., 2020; Cabedo et al., 2021).

In this paper, we aim to provide an overview of the chemical mechanisms associated with the post-impact synthesis starting from formamide - a prebiotic feedstock or intermediate. Formamide contains all the essential biogenic elements: carbon, nitrogen, hydrogen, and oxygen, and it is the simplest representation of a peptide linkage. Several plausible endogenous sources of formamide have been identified in early planetary environments: the hydrolysis of HCN (Saladino et al., 2006), volcanic activity (Sponer et al., 2016), radioactivity (Adam et al., 2018) and reprocessing of either simple atmospheric mixtures [CH_4, NH_3, H_2O, H_2] (Miller, 1953), [CO, CO_2, N_2, NH_3, H_2, H_2O] (Abelson, 1956) or more complex molecules such as formaldehyde (Ferus et al., 2019) or HNCO (Ferus et al., 2018) as well as their various combinations (Rode, 1999; Saitta and Saija, 2014; Cassone et al., 2018; Sponer et al., 2020). Formamide has also been observed in the interstellar medium, in young stars (Schutte et al., 1999; Kahane et al., 2013) and in comets (Biver et al., 2014; Goesmann et al., 2015). In addition, extra-terrestrial synthesis (Cassone et al., 2018) and exogenous delivery from extra-terrestrial environments is a potential source of this compound on early planets - including young Earth, Mars and Venus.

We report a synergistic experimental (FTIR spectroscopy, GC-MS) and computational (*ab initio* molecular dynamics) investigation on the thermal treatment of formamide in presence of clays, meteoritic Fe-Ni grains and iron oxide, we summarise the mechanism and show the relevant reaction intermediates. Besides, with the aim of offering a general and unified chemical picture, our findings are discussed in the context of previous studies on the prebiotic synthesis of canonical nucleobases initiated either by direct chemical action of an impact plasma or by subsequent formamide-based thermal treatment.

2 MATERIALS AND METHODS

Experiments were designed to prove the existence of stable intermediates inspired by the various mechanisms proposed by Saladino et al. (2007). Many other mechanistic variants have been published by Springsteen, Krishnamurthy and others (Hudson et al., 2012; Wang et al., 2013a,b). The intermediates are predicted to be formed from formamide or a formamide-clay mixture during thermal treatment and the main purpose of this experimental approach was their detection *via* an absolute detection method such as the Fourier Transform Infrared (FTIR) spectroscopy.

2.1 Experiment

Simulation of formamide thermolysis in presence of iron-rich smectites and other materials explored in this study in hot post-impact environment was performed in vacuum sealed quartz tubes filled with pure formamide mixed with sodium montmorillonite (Na-clay, Kunimine Industries, Japan), ferruginous smectite (Fe-clay, Clay Repository of the Clay Mineral Society, Grand County, Washington, United States) and montmorillonite (CAS 1318-93-0, K10 powder, Sigma Aldrich); iron (III) oxide (CAS, 1309-37-1, Merck $< 5\,\mu$m, $> 96.0\%$) and iron-rich meteorite Campo del Cielo (Fe 94%, Ni 6%). **Supplementary Table S1** provides the elemental composition and mineralogy of the samples obtained by standard X-ray diffractometry. The scanning electron microscope (SEM) photography of the samples is shown in **Supplementary Figure S1**. As for thermolysis, we mixed 0.1 g of solid powder with 2.0 ml of formamide ($> 99.0\%$, Sigma Aldrich). The sealed 100 ml vessel was then evacuated up to 0.1 Torr and then filled with inert N_2 up to 500 Torr. The samples were then heated with a Kanthal wire up to 180°C for 60 min.

2.2 Detection by FTIR

After thermolysis, the sample gas phase was expanded into an evacuated (1×10^{-2} Torr) multipass cell to a pressure of about 0.5 Torr. The cell with an optical path of 12 m was connected to a high-resolution FTIR spectrometer (Bruker IFS 125HR, Bruker Optics, Germany). The spectrometer was equipped with a KBr beamsplitter and nitrogen cooled LN-MCT (Hg-Cd-Te) detector. The spectra were measured in the range 680–4,800 cm^{-1} at a resolution of 0.02 cm^{-1} with 300 scans co-added for each sample. Standard calibration measurements of pure gases (HCN, Messer Technogas, 186 ppm/He; CO, Linde Gas 5.3; CO_2, Linde Gas 5.3 and NH3, Linde Gas 3.8) was performed for quantification purposes.

2.3 Computational Techniques

The condensed-phase dehydration reaction of formamide was reproduced by using Born-Oppenheimer molecular dynamics simulations and state-of-the-art metadynamics (MetD) methods (Pietrucci and Saitta, 2015). The results were obtained by exploiting the software suite for electronic structure and *ab initio* molecular dynamics (AIMD) simulations CP2K (Hutter et al., 2014) in conjunction with PLUMED-2.3.3 (Tribello et al., 2014), a patch which allows for the execution of MetD simulations. A cubic super-cell of side equal to 14.9 Å has been built in order to reproduce the experimental density of 1.13 g/cm^3, since 45 formamide molecules (*i.e.*, 270 atoms) were simulated. As usual in such a model, periodic boundary conditions were applied along the three Cartesian directions. The temperature was kept fixed by means of the CSVR (Bussi et al., 2007) thermostat at values fluctuating around an average of 160°C. Albeit some recent findings have shown the relevance of Nuclear Quantum Effects (NQEs) in assisting simple proton transfer reactions in hydrogen-bonded liquids (Cassone, 2020), due to the presence of the history-dependent potential introduced by MetD the dynamics of nuclei was simulated classically using the Verlet algorithm. Wavefunctions of each atomic species were expanded in TZVP basis sets whereas the core electron interactions were treated by means of the Goedecker-Teter-Hutter pseudopotentials (Goedecker et al., 1996) using the GPW method (Krack, 2005; VandeVondele et al., 2005). A plane-wave cutoff of 400 Ry was imposed whereas a timestep for the nuclei dynamics of 0.5 fshas been adopted. The employed exchange-correlation DFT functional is the dispersion-corrected GGA functional PBE-D3 (Perdew et al., 1996; Grimme et al., 2010, 2011).

The MetD formalism here adopted employs the matrices of coordination numbers with the aim of defining a given molecular state and exploits two Collective Variables (CV), *S* and *Z*, on which the free energy surface (FES) is constructed. The former variable represents the progress along the chemical transformation whereas the latter the distance from an ideal pathway. During the calculations, the following parameters have been adopted for the coordination function (see Equation 3 of Pietrucci and Saitta (2015): N = 6, M = 12, $R^0_{SS'}$, Rs = 1.8 Å for S,S' = O,C,N, 1.5 Å for S=O,C,N, S' = H, and 1.4 Å for S=S' = H. The parameter λ has been set such that $\lambda D\ (R_k, R_{k,\,k'}) \approx 2.3$. The MetD potential was composed of Gaussians with widths $\sigma_s = 0.03$ and $\sigma_z = 0.10$ and heights of 3 kcal·mol^{-1} deposed every 50 fs.

Geometry optimization and frequency analysis of the covalent and non-covalent (hydrogen-bonded) formamide dimer were performed by means of the ORCA software (V4.1.0) (Frank, 2012; Neese, 2018) using the hybrid meta functional PW6B95-D3(BJ) (Zhao and Truhlar, 2005; Grimme et al., 2010, 2011) in gas phase. To speed up the calculations, resolution-of-identity (RI) (Weigend, 2002) and chain-of-spheres (COSX) (Izsák and Neese, 2011) approximations were used for Coulomb and exchange integrals, respectively. All calculations employed the def2-QZVP basis set (Weigend and Ahlrichs, 2005) along with the auxiliary basis set def2/J (Weigend, 2006). Before performing the frequency analysis, geometries were re-optimized using

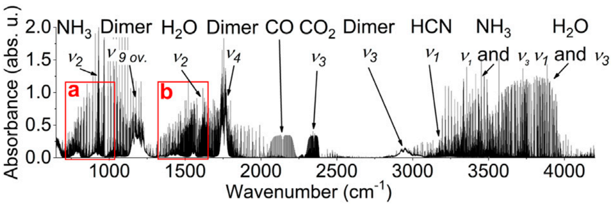

FIGURE 1 | FTIR spectrum of gaseous products formed from formamide thermolysis at 180°C in presence of Fe smectite. Boxes (a) and (b) frame the absorption features of 2-aminoacetonitrile (See **Figure 2A**) and formamidine (see **Figure 2B**), respectively. Band assignments including those for the non-covalent dimer of formamide are indicated (see **Figure 3A**); *ov*. stands for overtone.

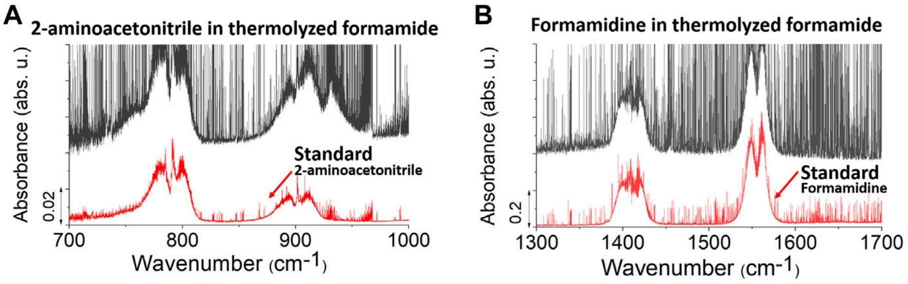

FIGURE 2 | Panel **(A)** Measured ν_9 and ν_8 spectral bands of gas-phase 2-aminoacetonitrile (*black trace*) following formamide thermolysis in presence of iron-rich smectite, compared with gas-phase spectra of neat 2-aminoacetonitrile (*red trace*). Panel **(B)** The ν_6 and ν_5 bands of formamidine following thermolysis for formamide and in a standard sample.

tighter convergence criteria (TightOpt keyword). Then, the frequency analysis within the harmonic approximation was performed at 160°C. Vibrational frequencies were checked in order to confirm that the molecular geometries corresponded to local minima of the potential energy surfaces. Gibbs free energies were calculated by adding the zero-point energy (ZPE), thermal and entropic corrections to the total electronic energy. The non-covalent formamide dimer was prepared such that its most stable form—the one forming the two N-H··· O hydrogen bonds—could be found during the geometry optimization.

3 RESULTS

3.1 FTIR Detection of Intermediates

Our FTIR survey has confirmed that major products released from liquid formamide heated to 180°C in the presence of clays are NH_3 and CO (Cataldo et al., 2009; Nguyen et al., 2011; Ferus et al., 2014), formed by decarbonylation, and HCN and H_2O, whose yield should dominate over NH_3 and CO (Nguyen et al., 2011; Ferus et al., 2014). Absorption spectra recorded after thermal treatment with Fe smectite are displayed in **Figure 1**.

However, our FTIR spectra also confirm synthesis of 2-aminoacetonitrile, formamidine (details provided in **Figure 2**) and of the non-covalently bound formamide dimer (see details provided by **Figure 3**). Together with HCN, aminoacetonitrile and formamidine represent central intermediates in the formamide-based thermally initiated origin of nucleobases and glycine in presence of meteoritic material residua or metal-rich clays in hot hydrothermal environment of craters (Saladino et al., 2018; Pastorek et al., 2019).

3.2 Computations

With the aim of quantifying the contribution supplied by the chemical environment in formamide towards its dehydration, *ab initio* molecular dynamics (AIMD) simulations coupled with advanced path-Collective-Variables metadynamics (MetD) have been performed in condensed (liquid) phase whilst free-energy estimates of the same reaction under gas-phase conditions are present in the literature (Saitta et al., 2015). As shown in **Figure 4**, the dehydration reaction in liquid formamide is hindered by a free-energy barrier height of 45 ± 3 $\text{kcal}\cdot\text{mol}^{-1}$. Although such a value may appear prohibitive, it is worth stressing here the fact that the same reaction exhibits a far larger barrier of about 70 $\text{kcal}\cdot\text{mol}^{-1}$ when reproduced under gas-phase conditions (Saitta et al., 2015). Moreover, since the experiments to be discussed in the following start from liquid samples of formamide either neat or mixed with clays, our estimate of the free-energy surface (FES) characterising such a reaction help quantifying the minimum energetic contribution carried by clays. In fact, it is straightforward that the free energy contributed by clays when mixed with liquid formamide accounts to at least 45 $\text{kcal}\cdot\text{mol}^{-1}$ for the dehydration reaction. Such a value is very close to that obtained in Pietrucci and Saitta (2015) simulating the same chemical transformation but in presence of liquid water (*i.e.*, by employing formamide as a solute in a water solvent). Mechanistically, in the absence of a clay, a formamide molecule cooperates with the solvent to release a water molecule, as shown by the atomistic pictures of the reaction in **Figure 4** (insets). Besides, HNCHOH is identified as a promising intermediate species during the conversion of formamide into H_2O and HCN, as it was also observed for the same reaction in an aqueous environment (Pietrucci and Saitta, 2015).

4 DISCUSSION

Impact plasma and residual post-impact heat are very important energy sources plausibly capable of changing the chemical inventory of early planets undergoing heavy bombardment. These factors may have created unique niches likely amenable also to energetically demanding reactions for prebiotic synthesis. Impact plasma chemistry and physics has become a subject of both laboratory and theoretical studies (Chyba and Sagan, 1992). Laser experiments summarized in our paper represent one of the approaches with their significant advantages as well as limitations, discussed in our recent studies and references therein, for example (Mohammadi et al., 2020; Ferus et al., 2020; Křivková et al., 2021). However, multiple other studies using different approaches have been also performed, such as target shock experiments (McCaffrey et al., 2014; Martins et al., 2013; Takeuchi et al., 2020) and references therein), shock tubes (Singh et al., 2020) and references therein) or even by quantum

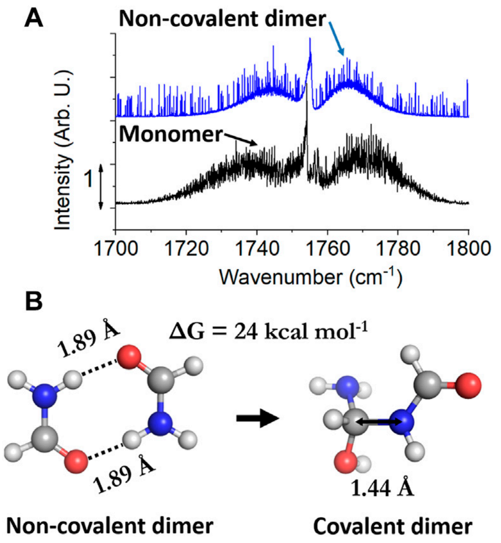

FIGURE 3 | Panel **(A)** Measured gas-phase spectrum of the ν_4 absorption bands of monomeric and non-covalent dimeric formamide formed by thermolysis in the presence of iron-rich smectite. The covalent formamide dimer is not detected. Panel **(B)** An indication of a quantum-chemically calculated reaction energy of 24 kcal·mol^{-1} restricting isomerisation of the non-covalent dimer to the covalent one.

chemical computations (Kroonblawd et al., 2019; Koziol and Goldman, 2015) and references therein).

The present study draws a unified picture of complex mechanisms of prebiotic synthesis initiated by impact plasma and thermochemistry in the post-impact environment in presence of iron-rich clays. Among elements such as Fe, Ni, Co, Al, Mn and Cr (Jarosewich, 1990), iron is an ubiquitous meteorite component. Iron can be present in the form of pure metal, alloy, a derived compound or as a constituent of various minerals (see (Jarosewich, 1990; Rubin, 1997; Brearley et al., 1998) and references therein). Therefore, investigation of formamide prebiotic chemistry in presence of Fe-smectites is addressed in this study. Prebiotic synthesis of nucleobases and glycine related to impact reprocessing of formamide can be summarised by two independent mechanisms following each other, as displayed in **Figure 5**. The whole process starts with impact plasma-assisted chemistry, as shown in **Figure 5A**, and follows with thermochemistry summarised in **Figure 5B**. For the sake of clarity, the results are also quantitatively summarised in **Table 1**. Intermediates of impact (A) or post-impact (B) chemistry directly detected in our experiments by means of absorption or emission spectroscopy and GC-MS are highlighted by green rectangles in **Figure 5**. The current investigation, as well as some previous studies (the list of references is provided alongside each particular scheme), combines in this way impact and post-impact chemistry of formamide toward a unified picture experimentally and theoretically supported.

Investigations focused on prebiotic chemistry initiated by an impact plasma (Civis et al., 2012; Ferus et al., 2012, 2015b; Ferus et al., 2014; Ferus et al., 2019) have reported that the origin of nucleobases, glycine and urea might start with the formation of radicals such as . CN, .H, :NH and . NH_2. FTIR spectroscopy has also given evidence of the formation of two intermediate species

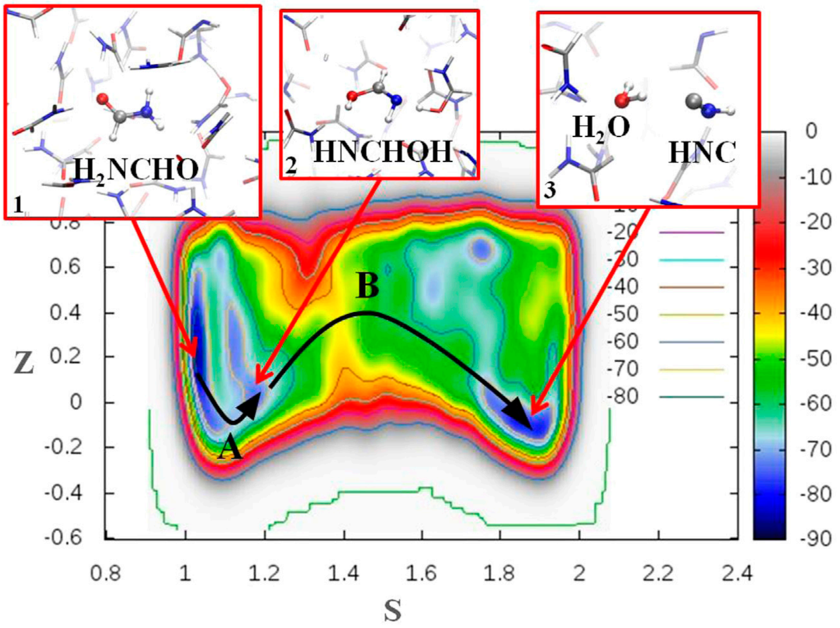

FIGURE 4 | Free-energy surface of the dehydration reaction of formamide in liquid formamide at 160 °C and in absence of any catalyst obtained *via ab initio* molecular dynamics and metadynamics simulations. As schematically indicated by the insets, values of the Collective Variable S ≈ 1 indicate a molecular state close to the reactants whereas values of S ≈ 2 indicate atomistic arrangement close to the products state. Free energies are expressed in kcal·mol^{-1}.

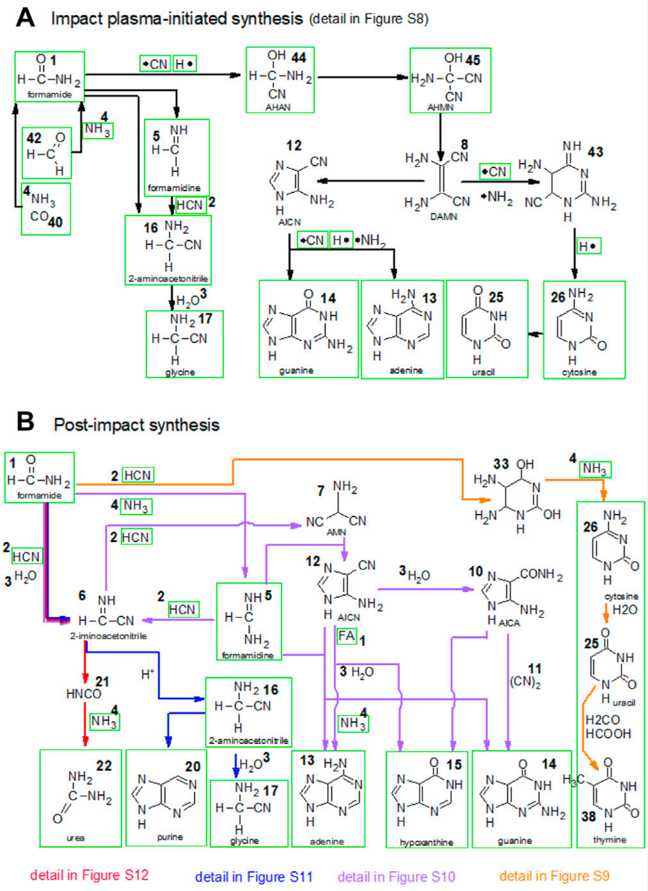

FIGURE 5 | Panel **(A)** Reaction scheme of radical chemistry responsible for the synthesis of nucleobases initiated directly by an impact plasma. Panel **(B)** Scheme for post-impact synthesis in impact craters starting with hot formamide. Both: Intermediates and products that are detected in the current and in previous studies are shown in green frames. Details including the description of each reaction pathway are given in the Supplementary Information figures as indicated by colours here. The figure was compiled from data published Ferus et al. (2014); Saladino et al. (2007); Ferus et al. (2015a); Ferus et al., 2019; Pastorek et al. (2019); Slavova and Enchev (2020); Yadav et al. (2020), and Hudson et al. (2012) and references therein.

associated with the radical-based mechanism displayed in **Figure 5A** (Ferus et al., 2012): 2-amino-2-hydroxy-acetonitrile (**44**, AHAN) and 2-amino-2-hydroxy-malononitrile (**45**, AHMN). In the direct impact synthesis, formamidine (**5**) - detected in this study also as an intermediate species in the formamide thermochemistry - results from the reaction of formamide (**1**) with ammonia (**4**) released by the decomposition of formamide in the plasma environment and suddenly created during the impact event. Formamidine (**5**) then reacts with HCN (**2**) to give rise to 2-iminoacetonitrile (**6**). 2-amino-2-hydroxy-acetonitrile (**44**, AHAN) and 2-amino-2-hydroxy-malononitrile (**45**, AHMN) hold a pivotal role in the thermal synthesis of nucleobases from formamide. For instance, formamide (**1**) may react with NH_3 to give formamidine (**5**), also detected in this investigation. Formamidine can then react with 2-aminomalononitrile (**7**) to AICN (**12**), which is a known precursor of adenine (**13**), hypoxanthine (**15**) and guanine (**14**). Formamidine can also react with HCN to give rise to 2-iminoacetonitrile (**6**). Besides, another way to produce 2-iminoacetonitrile (**6**) is from formamide and HCN. Then, 2-iminoacetonitrile (**6**) can either react with HNCO (**21**) and then urea (**22**), or can produce 2-aminoacetonitrile (**16**), which is a precursor of purine (**20**) and glycine (**17**).

Synthesis of nucleobases at ppmv (parts per million by volume) levels was observed not only starting from formamide, but also in experiments simulating impact plasma reprocessing atmospheres composed of NH_3:CO:H_2O (Ferus et al., 2017b) or formaldehyde aqueous solutions (Ferus, M. et al., 2019). In such a specific chemistry, formamide has been detected among other products and likely it does not serve as a starting compound but rather as a key prebiotic intermediate (**Figure 5A**). This aspect is quite important because impact plasma might have then served not only as an initiator of the nucleobases and glycine origin, but also as an endogenous source of formamide. The simplest approach to estimating the *de novo* impact synthesis yield is a linear scaling of experimental data (Curci et al., 2004; Rimmer et al., 2019; Mohammadi et al., 2020). We use the annual impact energy deposition estimated by Chyba et al. (Chyba and Sagan, 1992) (*i.e.*, 10^{20} J) for the end of the Hadean era. With this value, the yield of formamide per joule of delivered impact energy estimated by Ferus et al. (Ferus et al., 2017b) (3×10^{13} molecules/J) can then directly be translated into a global impact-formed formamide deposition equal to 2.24×10^5 tons per year. Together with the extra-terrestrial delivery of formamide, such a *de novo* synthesis might have represented its significant source. The relevance of the direct formamide synthesis can be illustrated on a Tunguska-scale impact event. As an example, let us apply the simulated impact-induced yields (Sutherland, 2016; Ferus et al., 2017b; Ferus et al., 2019) summarised for different experiments in **Table 1** for the estimation of formamide and nucleobases amounts produced by such large local impact event. It has been estimated that Tunguska provided energy on the order of 10^{17} J (Drobyshevski, 2009).

Then, it would be possible to expect that a few hundreds of tons of *de novo* formamide was deposited over an impact area of about 10^3 km^2 (area presumed to have been affected by the Tunguska impact) and led to the local synthesis and spread of a few ppm of all the canonical nucleobases in that environment. Linear scaling of this rational to the case of the Gale impact on Mars estimates a six orders of magnitude larger synthesis yield (Asphaug, 2008; Schwenzer et al., 2012). Similarly with formamide, direct synthesis of canonical nucleobases initiated by a simulated impact plasma has been observed in the case of the HCN-based chemistry as well (Ferus et al., 2020) and, similarly to the formamide case discussed here, HCN might have also been deposited locally (Todd and Öberg, 2020), a fact that could have created particularly favourable circumstances for prebiotic synthesis by post-impact chemistry (Sutherland, 2016). These estimates are of course very rough. Proper investigation including a chemical model is, however, beyond the scope of this paper. Also, significant amount of formamide and/or nucleobases produced by impacts does not wholly overcome the classical problems in prebiotic chemistry, such as how the chemical complexity increased from prebiotic molecules through simple organics to biopolymers, how interfaces for selection and concentration of more dilute solutions were provided and what created physical and chemical gradients and supported fluxes or cycles in the environment (Hazen and Sverjensky, 2010; Powner and Sutherland, 2011). For example, (Oró, 1961) described synthesis of adenine under primitive Earth conditions and (Stern et al., 2015) gives evidence for indigenous nitrogen in sedimentary and aeolian deposits, which implies that the early martian atmosphere may have been N-rich and thus favourable for the here-described synthesis as well. On the other hand, it has been suggested that HCN might have been accumulated in ferrocyanides (Sasselov et al., 2020), and formamide - due to its low volatility and sufficient stability - might have been concentrated in the hot-dry-wet cycle of craters in lagoons *et similia* (Miyakawa et al., 2002). Both mechanisms are well related to the typical environments of impact craters. It is expected that the residual post-impact heat supported hydrothermal activity for several hundreds thousands years (Schwenzer et al., 2012) and may have harboured a rich thermochemistry associated with the clays (Ehlmann et al., 2011; Pastorek et al., 2019) and resulting from the crater alteration or with what remains of the original material from the impactor. Importance of impact craters has suddenly been recognized when considering the well-known Gale crater on Mars, where organic molecules have been discovered by the Curiosity rover (Freissinet et al., 2015; Eigenbrode et al., 2018). Our recent investigations show that iron-rich smectites formed by hydrothermal alteration of basalts (as discovered in the case of the Nakhla ovoid structure (Chatzitheodoridis et al., 2014)) increases the thermolysis yields starting from formamide (Pastorek et al., 2019). Previous investigations conducted by Saladino, Di Mauro *et al.* also highlight the beneficial role of original meteoritic material (Saladino et al., 2013). Laboratory experiments have shown that those materials assist, during the formamide-based synthesis of nucleobases, amino acids and urea (Pastorek et al., 2019; Saladino et al., 2013). Some recent results are listed in **Table 1**, which summarises the nucleobases yields in a range of thermolysis as well as plasma experiments mimicking all stages of a meteorite impact events triggering potentially relevant prebiotic chemistry.

In the current work, detection of the formamide dimer, formamidine (**5**) and of 2-aminoacetonitrile (**16**) has allowed us to build up a unified picture also for the post-impact thermally-driven formamide-based prebiotic synthesis in craters, as shown in **Figure 5B**. Although the formamide dimer was previously detected by FTIR inspection of gas-phase formamide samples treated by laser spark (Ferus et al., 2012), the present study provides the first direct evidence of its origin from formamide upon heating. The heating provides energy to allow the system to pass a reaction barrier and form a dimer. The presence of a dimer has not been observed in standard formamide without any heating or the effect of a laser spark. With the aim of discerning among the possible forms of the formamide dimer, quantum-mechanical calculations of the free energy of the covalent and non-covalent (*i.e.*, hydrogen-bonded) dimer have been conducted at the hybrid meta PW6B95-D3(BJ)/def2-QZVP level at 160°C. Such a Gibbs free energy evaluation indicates that the non-covalent formamide dimer is quite more stable than the covalent one. In fact, the non-covalently bound formamide dimer is energetically preferred against the covalent one by a $\Delta G = 24\ \mathrm{kcal \cdot mol^{-1}}$. The conversion is schematically depicted in **Figure 3B**. In light of these fundamental quantum-mechanical information, we could speculate that the covalent dimer has not directly been detected possibly due, on the one hand, to the low volatility and limited occurrence of this intermediate in the liquid phase during the purine synthesis and, on the other, to its own supposed high reactivity with respect to the more stable hydrogen-bonded dimer. After all, indeed, dimerization of formamide to form a covalent bond represents the initial step in the synthesis of purines in a mechanism originally proposed by Yamada (Yamada and Okamoto, 1972; Yamada et al., 1978) and then revised by Saladino et al. (2007), as summarised in (c) and depicted in **Supplementary Figure S10** (Supplementary Information), which shows a specific mechanism of an intermediate synthesis finally resulting into the formation of cytosine, uracil and thymine.

The unified mechanism here proposed is ultimately confirmed by the detection—obtained *via* FTIR spectroscopy—of formamidine (**5**), an important intermediate in the synthesis of purine nucleobases such as adenine (**13**), hypoxanthine (**15**) and guanine (**14**), as shown in **Figure 5B**. Formamidine (**5**) is expected to result from the reaction of formamide (**1**) with ammonia (**4**). Formamidine (**5**) then reacts with HCN (**2**) to give rise to 2-iminoacetonitrile (**6**). Besides, it should be noted here that 2-iminoacetonitrile can be produced directly from formamide (**1**) by reaction with HCN (**2**). 2-iminoacetonitrile (**6**) then is able to react with HCN (**2**) to produce 2-aminomalononitrile (**7**, AMN). This latter, by combining with formamidine, leads to aminoimidazole-carboxamide (**12**, AICN). Further reaction of (**12**) with (**5**) is capable to synthesise adenine (**13**) and guanine (**15**). AICN (**12**) can also react with formamide (**1**) and NH_3 (**4**) to produce adenine (**13**) as an alternative. If, instead, AICN (**12**) reacts with formamide (**1**) and then water (**3**), hypoxanthine (**15**) is produced. Another possible pathway to guanine (**14**) passes through AICN (**12**), whose cyano- group is hydrolyzed to produce aminoimidazole-carboxamide (AICA, **10**). Further reaction with $(CN)_2$ (**11**) yields guanine (**14**). AICA represents also a possible precursor to hypoxanthine (**15**) (Ferus et al., 2014). 2-iminoacetonitrile (**6**) can also react with H^+ to give rise to 2-aminoacetonitrile (**16**), which was also detected in the current experiment. 2-aminoacetonitrile (**16**) either hydrolyses to glycine (**17**) or reacts with 5-aminoimidazole (**19**) to produce purine (**20**). The mentioned 2-iminoacetonitrile (**6**) can also be converted into HNCO (**21**) which, upon reaction with **4**, can yield urea (**22**) (Pastorek et al., 2019). Pyrimidine nucleobases can also be created from formamide, as described in (Saladino et al., 2007). Here, formamide (**1**) reacts with 2 HCN (**3**) and ammonia (**4**) to cytosine (**26**). Cytosine (**26**) then hydrolyses to uracil (**25**). Further reaction with formaldehyde (**42**) and formic acid (**46**) may even lead to thymine (**38**) (Barone et al., 2015).

TABLE 1 | Comparison of the results on formamide-based thermal prebiotic synthesis in the presence of meteorites (Saladino et al., 2013) and testing of the catalytic effect of clays (Pastorek et al., 2019), and formation from formamide (Ferus et al., 2017b; 2015b) and formaldehyde (Ferus et al., 2019) in impact-plasma simulations. Units are in ppm.

Experimental Composition	Adenine	Guanine	Cytosine	Uracil	Purine	Energy source	References
Neat Formamide	2	1		0.4	0.4	LIDB-simulated Impact Plasma	Ferus et al. (2015b)
H-clay	37	2	6	2	0.4	LIDB-simulated Impact Plasma	Ferus et al. (2015b)
NH_3:CO:H_2O H-clay	10	1	0.5	0.5		LIDB-simulated Impact Plasma	Ferus et al. (2017b)
Formaldehyde H-clay	15	1	0.5	0.5		LIDB-simulated Impact Plasma	Ferus. et al. (2019)
Neat Formamide	9	0.6	10	41	10,000	Heat	Pastorek et al. (2019)
NiFe	23	0.2	60	164	531	Heat	Pastorek et al. (2019)
Iron oxide	11	0.4	20	0	325	Heat	Pastorek et al. (2019)
Na-clay	30	17	16	10	1930	Heat	Pastorek et al. (2019)
H-clay	67	10	5	28	3,416	Heat	Pastorek et al. (2019)
Fe-clay	433	11	0.2	8	4,582	Heat	Pastorek et al. (2019)
Iron meteorites	211–400	0	57–120	238–278	1400–41,320	Heat	Saladino et al. (2013)
Iron-stony meteorites	103–107	0	30–32	300–345	1860–5,260	Heat	Saladino et al. (2013)
Chondrites	0–510	0	30–32	6–61	30–2,370	Heat	Saladino et al. (2013)
Achondrites	41–810	50–60	30–44	50–470	770–2,660	Heat	Saladino et al. (2013)

5 CONCLUSION

Our experiments probe a particular scenario and mechanism in the direct impact and post-impact chemistry of formamide. Direct impact radical-based synthesis can be initiated by the chemical action of an impact plasma with temperatures exceeding 5000 K on surface liquid formamide lagoons, but also for instance by reprocessing of formaldehyde (Ferus, M. et al., 2019), of reducing NH_3:CO:H_2O atmospheres (Ferus et al., 2017b), or even of hydrogen cyanide (Ferus et al., 2020). This kind of chemistry results in the one-pot origin of a few ppm of nucleobases (Ferus et al., 2015b). As reported in the current investigation, on longer timescales, *e.g.*, a few hundred thousand years, hydrothermal environments in impact craters characterised by the residual materials of meteorites (Saladino et al., 2013) or the formation of smectites (Pastorek et al., 2019)—especially when secondary iron-rich hydrous mineral phases are formed—can support a continuous nucleobase prebiotic synthesis by means of formamide thermochemistry and direct participation of 2-aminoacetonitrile and formamidine.

DATA AVAILABILITY STATEMENT

The original contributions presented in the study are included in the article/**Supplementary Material**, further inquiries can be directed to the corresponding authors.

AUTHOR CONTRIBUTIONS

MF designed the experiment and provided funding. AKn performed experimental work. AKř wrote the paper and provided its LaTex formatting. AP and JH performed experimental work and evaluated experimental data. LJ provided clays. EC provided and characterized the Nakhla meteorite. GC, KM, FS, JS and JES performed theoretical calculations and wrote the paper. All authors contributed to the article and approved the submitted version.

FUNDING

Financial support from the Czech Science Foundation (grant reg. no. 21-11366S) and ERDF/ESF "Centre of Advanced Applied Sciences" (No. CZ.02.1.01/0.0/0.0/16019/0000778) is greatly acknowledged. Besides, authors acknowledge financial support from the Joint Bilateral Project CNR-16964/CNR2211 between the Italian National Research Council (CNR) and the Czech Academy of Sciences (CAS).

SUPPLEMENTARY MATERIAL

The Supplementary Material for this article can be found online at: https://www.frontiersin.org/articles/10.3389/fspas.2022.882145/full#supplementary-material

REFERENCES

Abelson, P. H. (1956). Amino Acids Formed in Primitive Atmospheres. *Science* 124, 935. doi:10.1073/pnas.192568299

Abramov, O., and Mojzsis, S. J. (2016). Thermal Effects of Impact Bombardments on Noachian Mars. *Earth Planet. Sci. Lett.* 442, 108–120. doi:10.1016/j.epsl.2016.02.035

Adam, Z. R., Hongo, Y., Cleaves, H. J., II, Yi, R., Fahrenbach, A. C., Yoda, I., et al. (2018). Estimating the Capacity for Production of Formamide by Radioactive Minerals on the Prebiotic Earth. *Sci. Rep.* 8, 18483. doi:10.1038/s41598-017-18483-8

Asphaug, E. (2008). Critical Crater Diameter and Asteroid Impact Seismology. *Meteorit. Planet. Sci.* 43, 1075–1084. doi:10.1111/j.1945-5100.2008.tb00694.x

Barone, V., Latouche, C., Skouteris, D., Vazart, F., Balucani, N., Ceccarelli, C., et al. (2015). Gas-phase Formation of the Prebiotic Molecule Formamide: Insights from New Quantum Computations. *Mon. Notices R. Astronomical Soc.* 453, L31–L35. doi:10.1093/mnrasl/slv094

Biver, N., Bockelée-Morvan, D., Debout, V., Crovisier, J., Boissier, J., Lis, D. C., et al. (2014). Complex Organic Molecules in Comets C/2012 F6 (Lemmon) and C/

2013 R1 (Lovejoy): Detection of Ethylene Glycol and Formamide. *Astroomy. Astrophysic.* 566, L5. doi:10.1051/0004-6361/201423890

Bizzarri, B. M., Šponer, J. E., Šponer, J., Cassone, G., Kapralov, M., Timoshenko, G. N., et al. (2020). Meteorite-Assisted Phosphorylation of Adenosine under Proton Irradiation Conditions. *ChemSystemsChem* 2, e1900039. doi:10.1002/syst.201900039

Brearley, A. J., and Jones, R. H. (1998). Chondritic Meteorites. *Rev. Mineral. Geochem.* 36 (1), 3-01-3-398.

Bussi, G., Donadio, D., and Parrinello, M. (2007). Canonical Sampling through Velocity Rescaling. *J. Chem. Phys.* 126, 014101. doi:10.1063/1.2408420

Cabedo, V., Llorca, J., Trigo-Rodriguez, J. M., and Rimola, A. (2021). Study of Fischer-tropsch-type Reactions on Chondritic Meteorites. *Astronomy. Astrophys.* 650, A160. doi:10.1051/0004-6361/202039991

Cassone, G. (2020). Nuclear Quantum Effects Largely Influence Molecular Dissociation and Proton Transfer in Liquid Water under an Electric Field. *J. Phys. Chem. Lett.* 11, 8983–8988. doi:10.1021/acs.jpclett.0c02581

Cassone, G., Saija, F., Sponer, J., Sponer, J. E., Ferus, M., Krus, M., et al. (2018). Dust Motions in Magnetized Turbulence: Source of Chemical Complexity. *Astrophysic. J.* 866, L23. doi:10.3847/2041-8213/aae529

Cassone, G., Šponer, J., Saija, F., Di Mauro, E., Marco Saitta, A., and Šponer, J. E. (2017). Stability of $2',3'$ and $3',5'$ Cyclic Nucleotides in Formamide and in Water: a Theoretical Insight into the Factors Controlling the Accumulation of Nucleic Acid Building Blocks in a Prebiotic Pool. *Phys. Chem. Chem. Phys.* 19, 1817–1825. doi:10.1039/C6CP07993H

Cataldo, F., Patanè, G., and Compagnini, G. (2009). Synthesis of HCN Polymer from Thermal Decomposition of Formamide. *J. Macromol. Sci. Part A* 46, 1039–1048. doi:10.1080/10601320903245342

Chatzitheodoridis, E., Haigh, S., and Lyon, I. (2014). A Conspicuous Clay Ovoid in Nakhla: Evidence for Subsurface Hydrothermal Alteration on Mars with Implications for Astrobiology. *Astrobiology* 14, 651–693. doi:10.1089/ast.2013.1069

Chyba, C. F., Thomas, P. J., Brookshaw, L., and Sagan, C. (1990). Cometary Delivery of Organic Molecules to the Early Earth. *Science* 249, 366–373. doi:10.1126/science.11538074

Chyba, C., and Sagan, C. (1992). Endogenous Production, Exogenous Delivery and Impact-Shock Synthesis of Organic Molecules: an Inventory for the Origins of Life. *Nature* 355, 125–132. doi:10.1038/355125a0

Civiš, S., Ferus, M., Kubelík, P., Chernov, V. E., and Zanozina, E. M. (2012). Li I Spectra in the 4.65-8.33 Micron Range: High-Lstates and Oscillator Strengths. *Astronomy. Astrophys.* 545, A61. doi:10.1051/0004-6361/201219852

Civiš, S., Knížek, A., Ivanek, O., Kubelík, P., Zukalová, M., Kavan, L., et al. (2017). The Origin of Methane and Biomolecules from a CO_2 Cycle on Terrestrial Planets. *Nat. Astron.* 1, 721. doi:10.1038/s41550-017-0260-8

Curci, G., Visconti, G., Jacob, D. J., and Evans, M. J. (2004). Tropospheric Fate of Tunguska Generated Nitrogen Oxides. *Geophys. Res. Lett.* 31, a–n. doi:10.1029/2003GL019184

Damer, B., and Deamer, D. (2020). The Hot Spring Hypothesis for an Origin of Life. *Astrobiology* 20, 429–452. doi:10.1089/ast.2019.2045

Drobyshevski, E. M. (2009). *Tunguska-1908 and Similar Events in Light of the New Explosive Cosmogony of Minor Bodies*. Cornell University [arXiv]. doi:10.48550/arXiv.0903.3309

Ehlmann, B. L., Mustard, J. F., Murchie, S. L., Bibring, J.-P., Meunier, A., Fraeman, A. A., et al. (2011). Subsurface Water and Clay Mineral Formation during the Early History of Mars. *Nature* 479, 53–60. doi:10.1038/nature10582

Eigenbrode, J. L., Summons, R. E., Steele, A., Freissinet, C., Millan, M., Navarro-González, R., et al. (2018). Organic Matter Preserved in 3-Billion-Year-Old Mudstones at Gale Crater, Mars. *Science* 360, 1096–1101. doi:10.1126/SCIENCE.AAS9185

Erickson, T. M., Kirkland, C. L., Timms, N. E., Cavosie, A. J., and Davison, T. M. (2020). Precise Radiometric Age Establishes Yarrabubba, Western Australia, as Earth's Oldest Recognised Meteorite Impact Structure. *Nat. Commun.* 11, 300. doi:10.1038/s41467-019-13985-7

Ferus, M., Rimmer, P., Cassone, G., Knížek, A., Civiš, S., Šponer, J. E., et al. (2020). One-Pot Hydrogen Cyanide-Based Prebiotic Synthesis of Canonical Nucleobases and Glycine Initiated by High-Velocity Impacts on Early Earth. *Astrobiology* 20, 1–13. doi:10.1089/ast.2020.2231

Ferus, M., Civiš, S., Mládek, A., Šponer, J., Juha, L., and Šponer, J. E. (2012). On the Road from Formamide Ices to Nucleobases: IR-Spectroscopic Observation of a Direct Reaction between Cyano Radicals and Formamide in a High-Energy Impact Event. *J. Am. Chem. Soc.* 134, 20788–20796. doi:10.1021/ja310421z

Ferus, M., Knizek, A., Sponer, J. E., and Civis, S. (2015a). Radical Synthesis of Nucleic Bases from Formamide in Impact Plasma. *Chem. Listy* 109, 406

Ferus, M., Kubelík, P., Knížek, A., Pastorek, A., Sutherland, J., and Civiš, S. (2017a). High Energy Radical Chemistry Formation of HCN-Rich Atmospheres on Early Earth. *Sci. Rep.* 7, 6275. doi:10.1038/s41598-017-06489-1

Ferus, M., Laitl, V., Knizek, A., Kubelík, P., Sponer, J., Kára, J., et al. (2018). HNCO-based Synthesis of Formamide in Planetary Atmospheres. *Astronomy. Astrophysic.* 616, A150. doi:10.1051/0004-6361/201833003

Ferus, M., Michalčíková, R., Shestivská, V., Šponer, J., Šponer, J. E., and Civiš, S. (2014). High-Energy Chemistry of Formamide: A Simpler Way for Nucleobase Formation. *J. Phys. Chem. A* 118, 719–736. doi:10.1021/jp411415p

Ferus, M., Nesvorný, D., Šponer, J., Kubelík, P., Michalčíková, R., Shestivská, V., et al. (2015b). High-energy Chemistry of Formamide: A Unified Mechanism of Nucleobase Formation. *Proc. Natl. Acad. Sci. U.S.A.* 112, 657–662. doi:10.1073/pnas.1412072111

Ferus, M., Pietrucci, F., Saitta, A. M., Ivanek, O., Knížek, A., Kubelík, P., et al. (2019). Prebiotic Synthesis Initiated in Formaldehyde by Laser Plasma Simulating High-Velocity Impacts. *A&A* 626, A52. doi:10.1051/0004-6361/201935435

Ferus, M., Pietrucci, F., Saitta, A. M., Knížek, A., Kubelík, P., Ivanek, O., et al. (2017b). Formation of Nucleobases in a Miller-Urey Reducing Atmosphere. *Proc. Natl. Acad. Sci. U.S.A.* 114, 4306–4311. doi:10.1073/pnas.1700010114

Frank, N. (2012). *The ORCA Program System*, 2. Wiley Interdiscip Rev Comput Mol Sci, 73

Freissinet, C., Glavin, D. P., Mahaffy, P. R., Miller, K. E., Eigenbrode, J. L., Summons, R. E., et al. (2015). Organic Molecules in the Sheepbed Mudstone, Gale Crater, Mars. *J. Geophys. Res. Planets* 120, 495–514. doi:10.1002/2014JE004737

Goedecker, S., Teter, M., and Hutter, J. (1996). Separable Dual-Space Gaussian Pseudopotentials. *Phys. Rev. B* 54, 1703–1710. doi:10.1103/physrevb.54.1703

Goesmann, F., Rosenbauer, H., Bredehöft, J. H., Cabane, M., Ehrenfreund, P., Gautier, T., et al. (2015). Organic Compounds on Comet 67P/Churyumov-Gerasimenko Revealed by COSAC Mass Spectrometry. *Science* 349. doi:10.1126/science.aab0689

Gourier, D., Binet, L., Calligaro, T., Cappelli, S., Vezin, H., Bréhéret, J., et al. (2019). Extraterrestrial Organic Matter Preserved in 3.33 Ga Sediments from Barberton, South Africa. *Geochimica Cosmochimica Acta* 258, 207–225. doi:10.1016/J.GCA.2019.05.009

Grimme, S., Antony, J., Ehrlich, S., and Krieg, H. (2010). A Consistent and Accurate Ab Initio Parametrization of Density Functional Dispersion Correction (DFT-D) for the 94 Elements H-Pu. *J. Chem. Phys.* 132, 154104. doi:10.1063/1.3382344

Grimme, S., Ehrlich, S., and Goerigk, L. (2011). Effect of the Damping Function in Dispersion Corrected Density Functional Theory. *J. Comput. Chem.* 32, 1456–1465. doi:10.1002/jcc.21759

Hazen, R. M., Papineau, D., Bleeker, W., Downs, R. T., Ferry, J. M., McCoy, T. J., et al. (2008). Mineral Evolution. *Am. Mineralogist* 93, 1693–1720. doi:10.2138/am.2008.2955

Hazen, R. M., and Sverjensky, D. A. (2010). Mineral Surfaces, Geochemical Complexities, and the Origins of Life. *Cold Spring Harb. Perspect. Biol.* 2, a002162. doi:10.1101/cshperspect.a002162

Hudson, J. S., Eberle, J. F., Vachhani, R. H., Rogers, L. C., Wade, J. H., Krishnamurthy, R., et al. (2012). A Unified Mechanism for Abiotic Adenine and Purine Synthesis in Formamide. *Angew. Chem. Int. Ed.* 51, 5134–5137. doi:10.1002/anie.201108907

Hutter, J., Iannuzzi, M., Schiffmann, F., and VandeVondele, J. (2014). cp2k: Atomistic Simulations of Condensed Matter Systems. *WIREs Comput. Mol. Sci.* 4, 15–25. doi:10.1002/wcms.1159

Ivanov, B. A. (2008). "Size-Frequency Distribution of Asteroids and Impact Craters: Estimates of Impact Rate," in *Catastrophic Events Caused by Cosmic Objects*. Editors V. Adushkin and I. Nemchinov (Berlin-Heidelberg: Springer Berlin Heidelberg), 91–116.

Izsák, R., and Neese, F. (2011). An Overlap Fitted Chain of Spheres Exchange Method. *J. Chem. Phys.* 135, 144105. doi:10.1063/1.3646921

Jarosewich, E. (1990). Chemical Analyses of Meteorites: A Compilation of Stony and Iron Meteorite Analyses. *Meteoritics* 25, 323–337. doi:10.1111/j.1945-5100.1990.tb00717.x

Jenniskens, P., Wilson, M. A., Packan, D., Laux, C. O., Krüger, C. H., Boyd, I. D., et al. (1998). Meteors: A Delivery Mechanism of Organic Matter to the Early Earth. *Earth, Moon, Planets* 82/83, 57–70. doi:10.1023/A:1017017728166

Kahane, C., Ceccarelli, C., Faure, A., and Caux, E. (2013). Detection of Formamide, the Simplest but Crucial Amide, in a Solar-type Protostar. *ApJ* 763, L38. doi:10.1088/2041-8205/763/2/L38

Koziol, L., and Goldman, N. (2015). Prebiotic Hydrocarbon Synthesis in Impacting Reduced Astrophysical Icy Mixtures. *Astrophysc. J.* 803, 91. doi:10.1088/0004-637x/803/2/91

Krack, M. (2005). Pseudopotentials for H to Kr Optimized for Gradient-Corrected Exchange-Correlation Functionals. *Theor. Chem. Acc.* 114, 145–152. doi:10.1007/s00214-005-0655-y

Křivková, A., Petera, L., Laitl, V., Kubelík, P., Chatzitheodoridis, E., Lenža, L., et al. (2021). Application of a Dielectric Breakdown Induced by High-Power Lasers for a Laboratory Simulation of Meteor Plasma. *Exp. Astron* 51, 425–451. doi:10.1007/s10686-020-09688-3

Kroonblawd, M. P., Lindsey, R. K., and Goldman, N. (2019). Synthesis of Functionalized Nitrogen-Containing Polycyclic Aromatic Hydrocarbons and Other Prebiotic Compounds in Impacting glycine Solutions. *Chem. Sci.* 10, 6091–6098. doi:10.1039/C9SC00155G

Kuwahara, H., and Sugita, S. (2015). The Molecular Composition of Impact-Generated Atmospheres on Terrestrial Planets during the Post-accretion Stage. *Icarus* 257, 290–301. doi:10.1016/j.icarus.2015.05.007

Llorca, J., and Casanova, I. (1998). Formation of Carbides and Hydrocarbons in Chondritic Interplanetary Dust Particles: A Laboratory Study. *Meteorit. Planet. Sci.* 33, 243–251. doi:10.1111/j.1945-5100.1998.tb01629.x

Llorca, J., and Casanova, I. (2000). Reaction between H_2, CO, and H_2S over Fe, Ni Metal in the Solar Nebula: Experimental Evidence for the Formation of Sulfur-Bearing Organic Molecules and Sulfides. *Meteorit. Planet. Sci.* 35, 841–848. doi:10.1111/j.1945-5100.2000.tb01467.x

Martins, Z., Price, M. C., Goldman, N., Sephton, M. A., and Burchell, M. J. (2013). Shock Synthesis of Amino Acids from Impacting Cometary and Icy Planet Surface Analogues. *Nat. Geosci.* 6, 1045–1049. doi:10.1038/ngeo1930

McCaffrey, V. P., Zellner, N. E. B., Waun, C. M., Bennett, E. R., and Earl, E. K. (2014). Reactivity and Survivability of Glycolaldehyde in Simulated Meteorite Impact Experiments. *Orig. Life Evol. Biosph.* 44, 29–42. doi:10.1007/s11084-014-9358-5

McKay, C. P., and Stoker, C. R. (1989). The Early Environment and its Evolution on Mars: Implication for Life. *Rev. Geophys.* 27, 189–214. doi:10.1029/RG027i002p00189

Miller, S. L. (1953). A Production of Amino Acids under Possible Primitive Earth Conditions. *Science* 117, 528–529. doi:10.1126/SCIENCE.117.3046.528

Miyakawa, S., James Cleaves, H., and Miller, S. L. (2002). The Cold Origin of Life: A. Implications Based on the Hydrolytic Stabilities of Hydrogen Cyanide and Formamide. *Orig. life Evol. biosphere* 32, 195–208. doi:10.1023/A:1016514305984

Mohammadi, E., Petera, L., Saeidfirozeh, H., Knížek, A., Kubelík, P., Dudžák, R., et al. (2020). Formic Acid, a Ubiquitous but Overlooked Component of the Early Earth Atmosphere. *Chem. Eur. J.* 26, 12075–12080. doi:10.1002/chem.202000323

Šponer, J. E., Mohammadi, E., Petera, L., Saeidfirozeh, H., Knížek, A., Kubelík, P., Dudžák, R., et al. (2020). Formic Acid, a Ubiquitous but Overlooked Component of the Early Earth Atmosphere. *Chem. Eur. J.* 26, 12075–12080. doi:10.1002/chem.202000323

Neese, F. (2018). Software Update: the ORCA Program System, Version 4.0. *WIREs Comput. Mol. Sci.* 8, e1327. doi:10.1002/wcms.1327

Nguyen, V. S., Abbott, H. L., Dawley, M. M., Orlando, T. M., Leszczynski, J., and Nguyen, M. T. (2011). Theoretical Study of Formamide Decomposition Pathways. *J. Phys. Chem. A* 115, 841–851. doi:10.1021/jp109143j

Oberbeck, V., Marshall, J., and Schwartz, D. (1990). "A Model for Chemical Evolution of Life on Mars," in Lunar And Planetary Science Conference, 21

Oró, J. (1961). Mechanism of Synthesis of Adenine from Hydrogen Cyanide under Possible Primitive Earth Conditions. *Nature* 191, 1193–1194. doi:10.1038/1911193a0

Pastorek, A., Hrnčířová, J., Jankovič, L., Nejdl, L., Civiš, S., Ivanek, O., et al. (2019). Prebiotic Synthesis at Impact Craters: the Role of Fe-Clays and Iron Meteorites. *Chem. Commun.* 55, 10563–10566. doi:10.1039/C9CC04627E

Patel, B. H., Percivalle, C., Ritson, D. J., Duffy, C. D., and Sutherland, J. D. (2015). Common Origins of RNA, Protein and Lipid Precursors in a Cyanosulfidic Protometabolism. *Nat. Chem.* 7, 301–307. doi:10.1038/NCHEM.2202

Perdew, J. P., Burke, K., and Ernzerhof, M. (1996). Generalized Gradient Approximation Made Simple. *Phys. Rev. Lett.* 77, 3865–3868. doi:10.1103/PhysRevLett.77.3865

Pietrucci, F., and Saitta, A. M. (2015). Formamide Reaction Network in Gas Phase and Solution via a Unified Theoretical Approach: Toward a Reconciliation of Different Prebiotic Scenarios. *Proc. Natl. Acad. Sci. U.S.A.* 112, 15030–15035. doi:10.1073/pnas.1512486112

Powner, M., Sutherland, J., and Szostak, J. (2011). *The Origins of Nucleotides*, 2011. Synlett, 1956–1964. doi:10.1055/s-0030-1261177

Powner, M. W., and Sutherland, J. D. (2011). Prebiotic Chemistry: a New Modus Operandi. *Phil. Trans. R. Soc. B* 366, 2870–2877. doi:10.1098/rstb.2011.0134

Rimmer, P. B., Ferus, M., Waldmann, I. P., Knížek, A., Kalvaitis, D., Ivanek, O., et al. (2019). Identifiable Acetylene Features Predicted for Young Earth-like Exoplanets with Reducing Atmospheres Undergoing Heavy Bombardment. *Astrophys. J.* 888, 21. doi:10.3847/1538-4357/ab55e8

Rode, B. M. (1999). Peptides and the Origin of Life1. *Peptides* 20, 773–786. doi:10.1016/S0196-9781(99)00062-5

Rotelli, L., Trigo-Rodríguez, J. M., Moyano-Cambero, C. E., Carota, E., Botta, L., Di Mauro, E., et al. (2016). The Key Role of Meteorites in the Formation of Relevant Prebiotic Molecules in a Formamide/water Environment. *Sci. Rep.* 6, 38888. doi:10.1038/srep38888

Rubin, A. E. (1997). Mineralogy of Meteorite Groups. *Meteorit. Planet. Sci.* 32, 231–247. doi:10.1111/j.1945-5100.1997.tb01262.x

Ryder, G. (2002). Mass Flux in the Ancient Earth-Moon System and Benign Implications for the Origin of Life on Earth. *J. Geophys. Res. Planets* 107, 1583. doi:10.1029/2001je001583

Saitta, A. M., and Saija, F. (2014). Miller Experiments in Atomistic Computer Simulations. *Proc. Natl. Acad. Sci. U.S.A.* 111, 13768–13773. doi:10.1073/pnas.1402894111

Saitta, A. M., Saija, F., Pietrucci, F., and Guyot, F. (2015). Reply to Bada and Cleaves: Ab Initio Free-Energy Landscape of Miller-like Prebiotic Reactions. *Proc. Natl. Acad. Sci. U.S.A.* 112, E343–E344. doi:10.1073/pnas.1421035112

Saladino, R., Botta, G., Bizzarri, B. M., Di Mauro, E., and Garcia Ruiz, J. M. (2016). A Global Scale Scenario for Prebiotic Chemistry: Silica-Based Self-Assembled Mineral Structures and Formamide. *Biochemistry* 55, 2806–2811. doi:10.1021/acs.biochem.6b00255

Saladino, R., Botta, G., Delfino, M., and Di Mauro, E. (2013). Meteorites as Catalysts for Prebiotic Chemistry. *Chem. Eur. J.* 19, 16916–16922. doi:10.1002/chem.201303690

Saladino, R., Botta, G., Pino, S., Costanzo, G., and Di Mauro, E. (2012). Genetics First or Metabolism First? the Formamide Clue. *Chem. Soc. Rev.* 41, 5526–5565. doi:10.1039/c2cs35066a

Saladino, R., Botta, L., and Di Mauro, E. (2018). The Prevailing Catalytic Role of Meteorites in Formamide Prebiotic Processes. *Life* 8. doi:10.3390/life8010006

Saladino, R., Crestini, C., Ciciriello, F., Costanzo, G., and Di Mauro, E. (2007). Formamide Chemistry and the Origin of Informational Polymers. *Chem. Biodiverse.* 4, 694–720. doi:10.1002/cbdv.200790059

Saladino, R., Crestini, C., Ciciriello, F., Di Mauro, E., and Costanzo, G. (2006). Origin of Informational Polymers. *J. Biol. Chem.* 281, 5790–5796. doi:10.1074/jbc.M512545200

Sasselov, D. D., Grotzinger, J. P., and Sutherland, J. D. (2020). The Origin of Life as a Planetary Phenomenon. *Sci. Adv.* 6, eaax3419. doi:10.1126/sciadv.aax3419

Schlichting, H. E., Warren, P. H., and Yin, Q.-Z. (2012). The Last Stages of Terrestrial Planet Formation: Dynamical Friction and the Late Veneer. *Astrophys. J* 752, 8. doi:10.1088/0004-637X/752/1/8

Schutte, W. A., Boogert, A. C. A., Tielens, A., Whittet, D. C. B., Gerakines, P. A., Chiar, J. E., et al. (1999). Weak Ice Absorption Features at 7.24 and 7.41 Mu M in the Spectrum of the Obscured Young Stellar Object W 33A. *Astronomy. Astrophys.* 343, 966

Schwenzer, S. P., Abramov, O., Allen, C. C., Bridges, J. C., Clifford, S. M., Filiberto, J., et al. (2012). Gale Crater: Formation and Post-impact Hydrous Environments. *Planet. Space Sci.* 70, 84–95. doi:10.1016/j.pss.2012.05.014

Singh, S. V., Vishakantaiah, J., Meka, J. K., Sivaprahasam, V., Chandrasekaran, V., Thombre, R., et al. (2020). Shock Processing of Amino Acids Leading to Complex Structures-Implications to the Origin of Life. *Molecules* 25, 5634. doi:10.3390/molecules25235634

Slavova, S., and Enchev, V. (2020). Self-catalytic Mechanism of Prebiotic Reactions: From Formamide to Purine Bases. *Int. J. Quantum Chem.* 120, e26362. doi:10.1002/qua.26362

Šponer, J. E., Šponer, J., Nováková, O., Brabec, V., Šedo, O., Zdráhal, Z., et al. (2016). Emergence of the First Catalytic Oligonucleotides in a Formamide-Based Origin Scenario. *Chem. Eur. J.* 22, 3572–3586. doi:10.1002/chem.201503906

Šponer, J. E., Szabla, R., Góra, R. W., Saitta, A. M., Pietrucci, F., Saija, F., et al. (2016). Prebiotic Synthesis of Nucleic Acids and Their Building Blocks at the Atomic Level - Merging Models and Mechanisms from Advanced Computations and Experiments. *Phys. Chem. Chem. Phys.* 18, 20047–20066. doi:10.1039/c6cp00670a

Stern, J. C., Sutter, B., Freissinet, C., Navarro-González, R., McKay, C. P., Archer, P. D., Jr., et al. (2015). Evidence for Indigenous Nitrogen in Sedimentary and Aeolian Deposits from the Curiosity Rover Investigations at Gale Crater, Mars. *Proc. Natl. Acad. Sci. U. S. A.* 112, 4245–4250. doi:10.1073/pnas.1420932112

Sutherland, J. D. (2017). Opinion: Studies on the Origin of Life - the End of the Beginning. *Nat. Rev. Chem.* 1, 12. doi:10.1038/s41570-016-0012

Sutherland, J. D. (2016). The Origin of Life-Out of the Blue. *Angew. Chem. Int. Ed.* 55, 104–121. doi:10.1002/anie.201506585

Takeuchi, Y., Furukawa, Y., Kobayashi, T., Sekine, T., Terada, N., and Kakegawa, T. (2020). Impact-induced Amino Acid Formation on Hadean Earth and Noachian Mars. *Sci. Rep.* 10, 66112. doi:10.1038/s41598-020-66112-8

Todd, Z. R., and Öberg, K. I. (2020). Cometary Delivery of Hydrogen Cyanide to the Early Earth. *Astrobiology* 20, 1109–1120. doi:10.1089/ast.2019.2187

Tribello, G. A., Bonomi, M., Branduardi, D., Camilloni, C., and Bussi, G. (2014). PLUMED 2: New Feathers for an Old Bird. *Comput. Phys. Commun.* 185, 604–613. doi:10.1016/j.cpc.2013.09.018

VandeVondele, J., Krack, M., Mohamed, F., Parrinello, M., Chassaing, T., and Hutter, J. (2005). QUICKSTEP: Fast and Accurate Density Functional Calculations Using a Mixed Gaussian and Plane Waves Approach. *Comput. Phys. Commun.* 167, 103–128. doi:10.1016/j.cpc.2004.12.014

Wang, J., Gu, J., Nguyen, M. T., Springsteen, G., and Leszczynski, J. (2013a). From Formamide to Adenine: a Self-Catalytic Mechanism for an Abiotic Approach. *J. Phys. Chem. B* 117, 14039–14045. doi:10.1021/jp409296k

Wang, J., Gu, J., Nguyen, M. T., Springsteen, G., and Leszczynski, J. (2013b). From Formamide to Purine: An Energetically Viable Mechanistic Reaction Pathway. *J. Phys. Chem. B* 117, 2314–2320. doi:10.1021/jp311423q

Weigend, F. (2002). A Fully Direct RI-HF Algorithm: Implementation, Optimised Auxiliary Basis Sets, Demonstration of Accuracy and Efficiency. *Phys. Chem. Chem. Phys.* 4, 4285–4291. doi:10.1039/B204199P

Weigend, F. (2006). Accurate Coulomb-Fitting Basis Sets for H to Rn. *Phys. Chem. Chem. Phys.* 8, 1057–1065. doi:10.1039/b515623h

Weigend, F., and Ahlrichs, R. (2005). Balanced Basis Sets of Split Valence, Triple Zeta Valence and Quadruple Zeta Valence Quality for H to Rn: Design and Assessment of Accuracy. *Phys. Chem. Chem. Phys.* 7, 3297–3305. doi:10.1039/b508541a

Xu, J., Tsanakopoulou, M., Magnani, C. J., Szabla, R., Šponer, J. E., Šponer, J., et al. (2017). A Prebiotically Plausible Synthesis of Pyrimidine β-ribonucleosides and Their Phosphate Derivatives Involving Photoanomerization. *Nat. Chem.* 9, 303–309. doi:10.1038/NCHEM.2664

Yadav, M., Kumar, R., and Krishnamurthy, R. (2020). Chemistry of Abiotic Nucleotide Synthesis. *Chem. Rev.* 120, 4766–4805. doi:10.1021/acs.chemrev.9b00546

Yamada, H., Hirobe, M., Higashiyama, K., Takahashi, H., and Suzuki, K. T. (1978). Reaction Mechanism for Purine Ring Formation as Studied by 13C-15N Coupling. *Tetrahedron Lett.* 19, 4039–4042. doi:10.1016/S0040-4039(01)95134-2

Yamada, H., and Okamoto, T. (1972). A One-step Synthesis of Purine Ring from Formamide. *Chem. Pharm. Bull.* 20, 623–624. doi:10.1248/cpb.20.623

Zhao, Y., and Truhlar, D. G. (2005). Design of Density Functionals that Are Broadly Accurate for Thermochemistry, Thermochemical Kinetics, and Nonbonded Interactions. *J. Phys. Chem. A* 109, 5656–5667. doi:10.1021/jp050536c

Conflict of Interest: The authors declare that the research was conducted in the absence of any commercial or financial relationships that could be construed as a potential conflict of interest.